

Effect of Different Loads on Fatigue Strength of 1040 Steel Materials After Design and Manufacturing of Rotating-Bending Fatigue Test Device

Hakan GÖKMEŞE and Onur GÖK

¹Konya Necmettin Erbakan University, Seydişehir Ahmet Cengiz Faculty of Engineering, Dept. of Mechanical Eng., 42370, Seydişehir-Konya, Turkey

²Konya Necmettin Erbakan University, Seydişehir Vocational School, Dept. of Machine and Metal Technologies., 42370, Seydişehir-Konya, Turkey

Corresponding Author: Hakan GÖKMEŞE

ABSTRACT : In this study, after the design of a new fatigue test device, the manufacturing of the device was carried out. In the virtual environment, appropriate machine elements and connections were made for the fatigue test device. For the manufacturing of the fatigue testing device, considering economic factors and efficiencies, DEG Drive brand 2-pole MS 90L electric motor that had output power 2.2 kW and output speed 2840 RPM and that had aluminum housing and 1-2 alternating current (AC) was used. Fatigue in the machine elements as a destructive test is known as fracture or rupture as a result of repeated stress under yield strength. In terms of conventional calculation methods, strength calculations can be made according to elasticity theory, taking into account design, conditions of use, and other effects. However, in terms of fatigue strength, breaks that occur with cyclic stresses applied depending on time indicate that these calculations are not sufficient. In calculations performed under the influence of repetitive dynamic load, fatigue strength must be taken into account. In order for the fatigue test device to work safely, the appropriate materials were selected, the strength was calculated, and the dimensions of the sample holder collets were determined. After the manufacturing of the fatigue test device, fatigue strength, the number of cycles, and fracture form of 1040 steel material were examined under applied different loads.

KEYWORDS Fatigue, fatigue device, design

Date of Submission: 11-11-2020

Date of acceptance: 26-11-2020

I. INTRODUCTION

One of the important stages for designers during machine design and manufacturing is also material selection and sizing stage. This stage directly affects the ergonomic structure of the machine and production costs (e.g., the amount of material used, labor, etc.). Many materials in the industry are subjected to cyclic stress or shape changes well below their tensile strength. When a single static stress is applied, parts subjected to repetitive or cyclic loads break off at a stress well below the stress they can withstand. These breakings are called fatigue fractures. The usability of the material can be better decided by examining its fatigue properties. Damage occurring in this way is called fatigue. S-N (Wöhler) curves are usually used to calculate the fatigue properties of the material [1-4].

Different models have been proposed to estimate fatigue strength. Most of the studies that refer to stresses are based on S-N diagrams or Wöhler curves, which represent stress levels. Over the years, the effect of different parameters such as stress rate, loading frequency, and uncertainty about load position have been investigated in these models [5-7].

Damage to engineering materials emerges when a crack occurs. This crack grows erratically and causes the material to break completely. Fatigue damage also occurs at cyclic stress levels much lower than the tensile strength applied to the material. The fatigue resistance of a structural part is affected by mechanical, metallurgical, and environmental variables. Fatigue is the primary cause of 80-90% of all engineering damages [8]. The properties and application areas of an engineering material can be specified by two main design approaches. First, in the total life approach, there are no defects in the material; when stress or stress life curves

are used, the material life can be estimated based on design loads. In the other approach, when the defect is called as tolerant, it is assumed that the starting material already has defects, and with the applied load, the fault will grow towards the fracture. In this case, the fatigue life can be calculated based on how long it takes for the crack to spread from the initial size to the critical size [9].

The fatigue process is three stages: The occurrence of initial fatigue damage leading to the onset of crack, becoming of the remaining cross-section too weak to carry the applied loads as a result of the progression of the crack, and sudden fracture of the remaining cross-section. Due to such a non-uniform microstructure that the materials have, the stresses are dispersed in a non-uniform way. Areas where stresses are severe are usually the points where fatigue damage begins. Conventionally, the total fatigue life of the material is taken into account in the design of engineering structures. But, under operating conditions, machine elements may contain defects such as scratches, impurities, and cracks. In the structural element operating under dynamic loads, fatigue cracking can begin from these defects. In general, factors affecting fatigue behavior of materials can be listed as stress concentrations, material size and surface parameters [10-13].

In this study, the design and manufacture of a fatigue test device were carried out for materials that had cylindrical cross-section and especially metal character. As a result of design and manufacturing studies, fatigue properties were examined on 1040 steel test samples under the influence of different loads and the S-N curve was drawn.

II. DESIGN AND MANUFACTURING

In terms of destructive testing of materials, fatigue test equipment can be designed and manufactured in different types, such as axial and environmental tilt. In terms of design and manufacture of fatigue test device; a fatigue test device driven by a motor on a common chassis and carrying a peripheral tilt unit within it was considered. In this context, the device can be specified as a “built-in (encastre) beam” type fatigue test device. In this type of test device, the standard test sample is connected from its head part and the rotation effect is provided by a motor. On the other side, the test sample is attached to a bearing shaft from the other side with the help of apparatus, and rotation of it in a rigid way is ensured. In this case, the number of cycles in which the test sample is broken or not broken against the bending stress under the effect of the applied load can be calculated with the necessary measurements. The fatigue test device designed in a virtual environment in accordance with the specified information is shown in Figure 1.

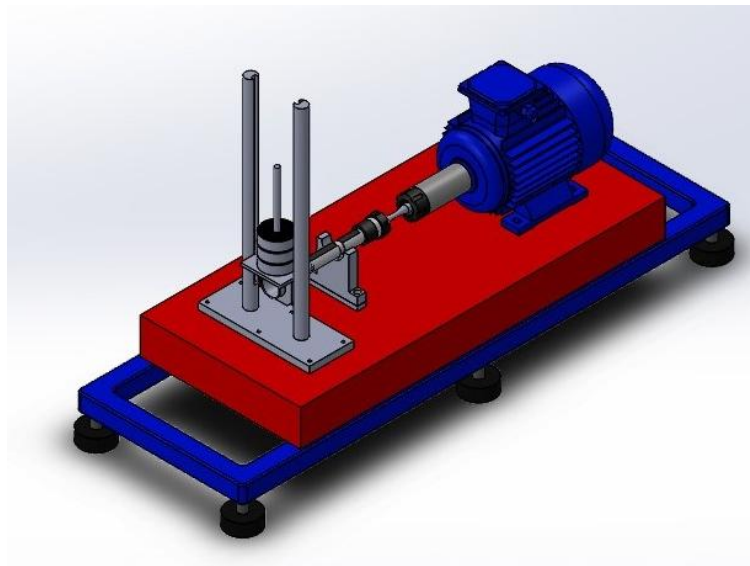


Figure 1. Designed fatigue test device

Considering the design and manufacture of the fatigue test device, an electric motor with 2.2 kW and 2840 rpm values was mounted firmly in the body of the test device. Collet holder connection is made to the shaft on the motor side and to the opposite side. Considering the sample connection area in the fatigue test device, a load application area is designed for the targeted bending stress. In this context, different loading operations can be performed on the load application area; this image is shown in Figure 2.

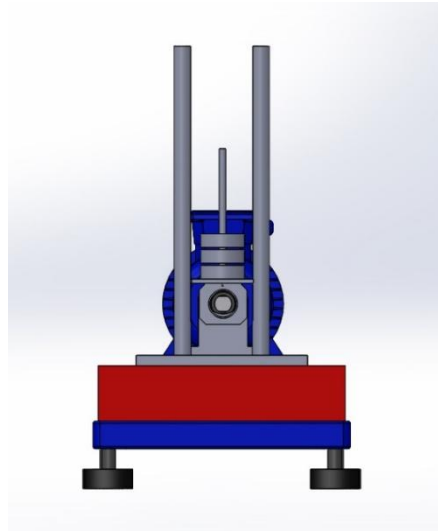


Figure 2. Bending stress effect and load application area

III. RESULTS AND DISCUSSION

In materials, under the influence of cyclic stresses applied under yield strength, the behavior of breaking or fracturing is very important because it is known that materials do not always work under the influence of constant or static loads. Therefore, the working conditions of the materials are encountered in the presence of continuous cyclic stresses such as rotation, bending and vibration. As a result of this situation, fatigue testing is performed as a destructive testing method. In materials, fatigue strength, limit, and life can be determined.

Given the information specified in terms of the fatigue test device, the cyclic stress in the material is applied as rotation with the help of a motor. Mainly in applications of fatigue experiment, 1500 rpm and 3000 rpm motors are preferred. Thanks to its high environmental speed, the motor with 3000 rpm can transfer the desired force to the sample at maximum speed. In terms of design and manufacturing of the test device, a 3000 rpm motor was used in studies. If motor power is shown with P_m , motor efficiency with η_m , shaft input power with P_i , shaft output power with P_o , and total device efficiency with η_{tot} , it should be that $P_m * \eta_m > P_i$ and $P_o = \eta_{tot} * P_i$. The efficiency of roller bearings is selected as $\eta_y = 0.97$.

Accordingly, from the input power (P_i) formula;

$$P_i = \frac{P_o}{\eta_{tot}} = \frac{1.5}{0.97} \rightarrow P_i = 1.546 \text{ kW was found.} \quad (1)$$

Table 1. Properties of the electric motor

Rated Speed (dev/dak)	Input Speed (dev/dak)	Type	Power (kW)	Yield
2840	3000	MS 90L 1-2	2.2	0.81

The properties of the electric motor used in the production of fatigue test device are shown in Table 1. The collet holder shown in Figure 3 was selected to squeeze a test sample with 15 mm diameter for the opposite side of the motor. In order for the collet holder used to rotate smoothly on the bearing, a smooth circular surface was formed by the turning on the shaft at the back. The collet on the motor part was selected in the diameter of the shaft connected to the motor. The collet at the opposite of the motor, on the other hand, was selected depending on the collet holder and the experimental sample (Figure 4).

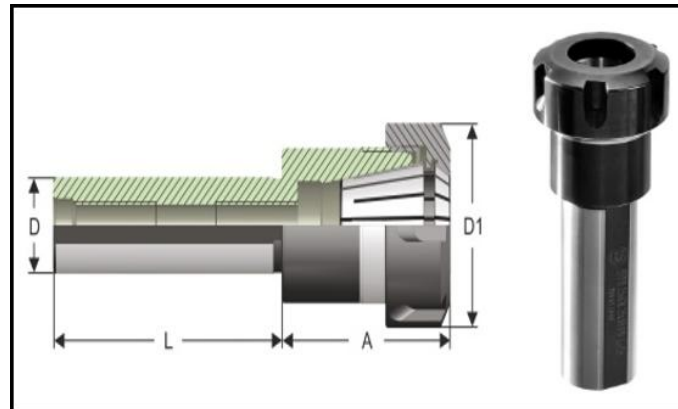


Figure 3. Collet holder; $D=25\text{mm}$, $L=150\text{mm}$, $A=50\text{mm}$, $D1=42\text{mm}$

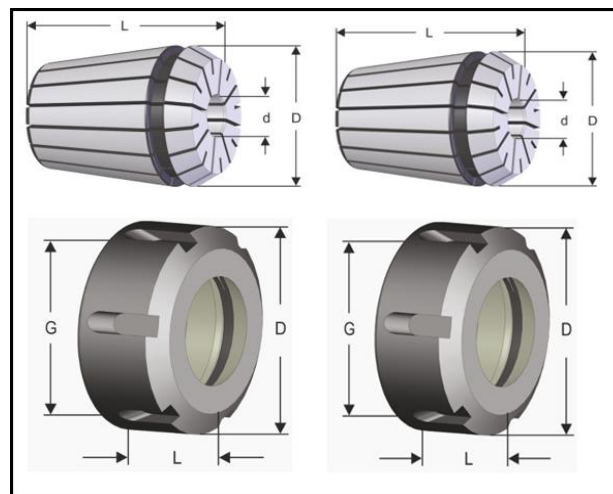


Figure 4. Collet head and caps;

- a) $D=50\text{mm}$, $d= 15\text{-}16\text{mm}$, $L=34\text{mm}$, b) $D=40\text{mm}$, $d=15\text{-}16\text{mm}$, $L=34\text{mm}$, c) $M40\times 1.5\text{mm}$, $D=52\text{mm}$, $L=30\text{mm}$, d) $G=M32\times 1.5\text{mm}$, $D=42\text{mm}$, $L=20\text{mm}$

Depending on the strength account, the loads to be used for the design and manufacture of the fatigue test device were placed at the farthest point to the test sample. The test loads used were selected considering the standard fatigue sample (figure 5a). Selected loads could be applied up to 25 kg during testing. The used load material was preferred as an iron-based alloy. The entire length of the standard test sample was 100 mm, the outer diameter of it was 15 mm, the length of its radius part was 50 mm, and the thinnest diameter in the center of it was 9 mm, and it was made of 1040 steel (Figure 5b). After the design studies conducted in the virtual environment, the manufacturing of the fatigue test device was carried out with the specified information (Figure 6).

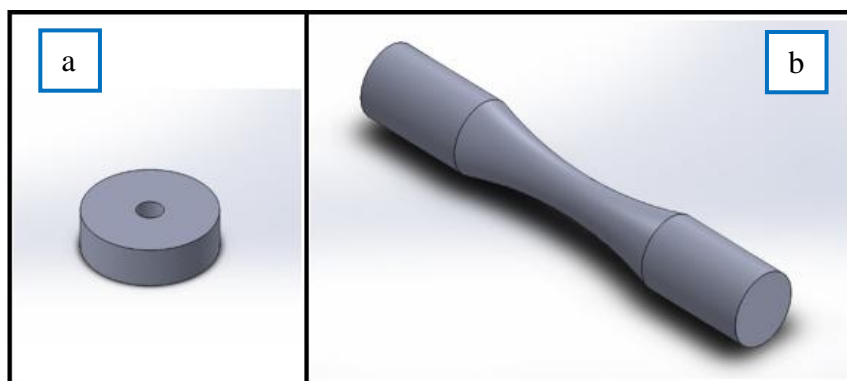


Figure 5. Fatigue test; a) Load, b) Standard test sample

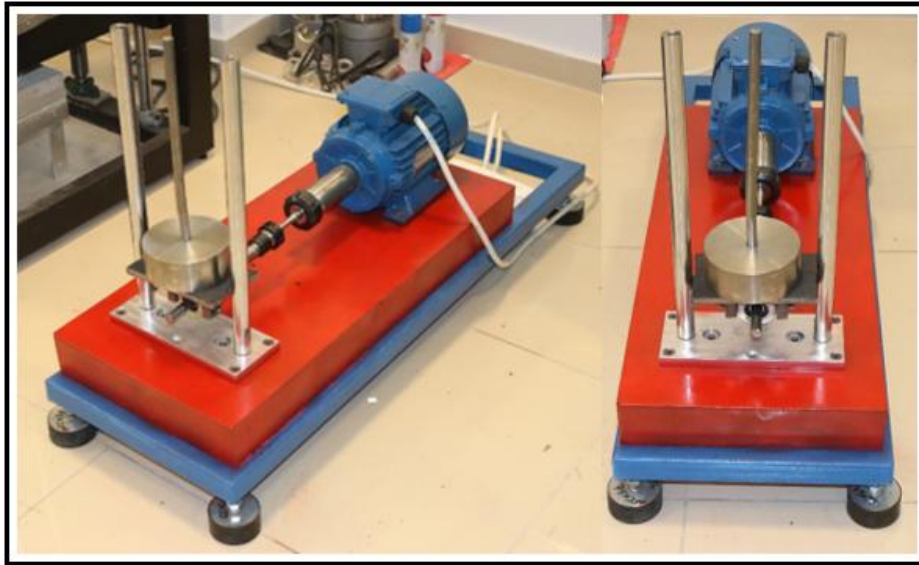


Figure 6. Fatigue testing device manufactured

For use in fatigue test experiments, data related to the fatigue stress were specified as follows, respectively; n : motor speed (rpm), d : shaft radius (mm), L : shaft length (mm), r : sample radius (mm), P : bending force (N), N : Power (Kw), M_e : bending moment (N.mm), M_b : torsion moment (N.mm), M_f : resultant moment (N.mm), σ y : fatigue strength (N. mm²). In addition, motor speed, shaft length, sample radius, power, and shaft radius were used as n : 2840 rpm, L : 250 mm, r : 4 mm, N : 2.2 Kw, and d : 12.5 mm, respectively.

Based on the formula given in Equation 2, the value of M_e was found as follows;

$$M_e = P.L \quad (2)$$

$$P = 25 \times 9.81 = 245.25 \text{ N}, L = 250 \text{ mm}$$

$$M_e = 245.25 \times 250$$

$$M_e = 61312.5 \text{ N.mm}$$

Based on the formula given in Equation 3, the value of M_b was found as follows;

$$M_b, \quad T = N/w \quad (3)$$

$$T = N/w \quad T = (2,2 \cdot 1000)/((2.\pi \cdot 2840)/60) \times 10^3 = 7397.34 \text{ N.mm}$$

$$T = P.r \quad T = 245.25 \times 4 = 981 \text{ N.mm}$$

$$M_b = 7397.34 - 981$$

$$M_b = 6416.34 \text{ N.mm}$$

Based on the formula given in Equation 4, the value of M_f was found as follows;

$$M_f = \sqrt{(M_e^2 + M_b^2)} \quad (4)$$

$$M_f = \sqrt{((61312.5)^2 + (6416.34)^2)}$$

$$M_f = 61647.32 \text{ N.mm}$$

Based on the formula given in Equation 5, the value of σ_y was found as follows;

$$\sigma_y = (Mf / \pi \cdot d^3) \cdot 32 \tag{5}$$

$$\sigma_y = (61647.32 / \pi \cdot 12,5^3) \cdot 32$$

$$\sigma_y = 321.50 \text{ N.mm}^2$$

Within the scope of the stated results; σ_y was applied as $\sigma_y = P \times 1.31 \text{ (N/mm}^2\text{)}$. In determining fatigue strength, this equation was preferred for use in experimental studies. After the design and manufacturing activities of the fatigue test device, the results of experimental studies performed using 1040 Steel materials under different loads are shown in Table 2.

Table 2. Steel material fatigue test results

Material	Load	Fatigue strength (N/mm ²)	Number of cycles	LogN
Ç1040	250	327.5	1363.2	3.13
Ç1040	200	262	2641.2	3.42
Ç1040	150	196.5	17182	4,23
Ç1040	100	131	21612.4	4.33
Ç1040	50	65.5	32745.2	4.51

As a result of a fatigue test, the S-N (Wöhler) curve shows the magnitude of the stress amplitude corresponding to the number of cycles in which a material is damaged. On this curve, usually, both the stress and the number of cycles can be given on logarithmic scales. In order to determine the cumulative damage or fatigue life of a mechanical part and to identify the loading history, the S-N (Wöhler) curve is quite important. Therefore, the S-N (Wöhler) curve obtained using steel material fatigue test results is shown in Figure 7. Figure 8 shows the fractured steel material as a result of the fatigue tests under different loads applied in experimental studies.

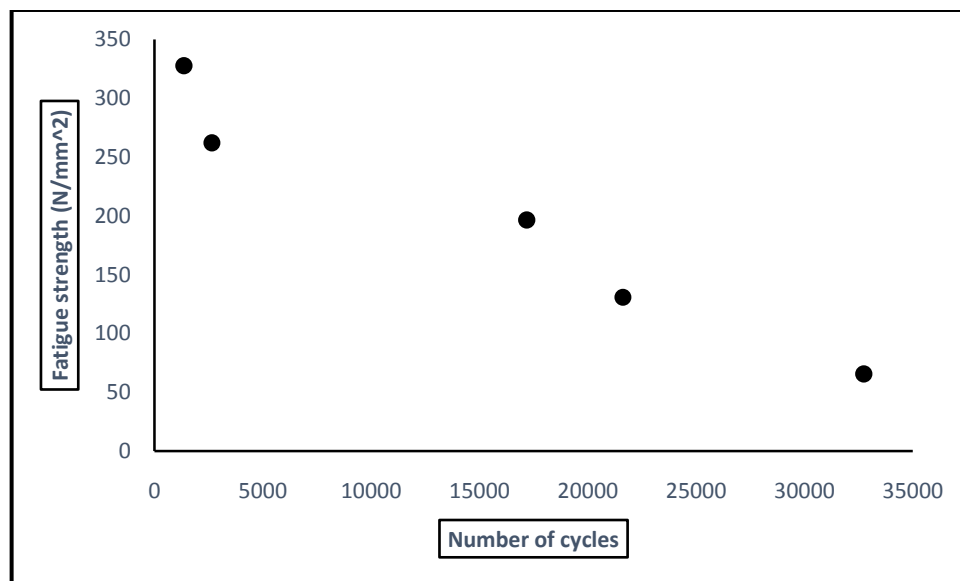


Figure 7.S-N curve after steel material fatigue test



Figure 8. Fatigue fracture zones of steel materials

IV. CONCLUSION

Fatigue tests are carried out to determine the fatigue life of machine elements operating under dynamic loads. In this study, in order to determine the fatigue behavior of metal-character materials and to obtain S-N curves, rotating bending fatigue test device was designed and manufactured. Variable loading values can be applied to the sample, while constant speed is used in the test device after its design and manufacture. After the manufacturing studies, it has been determined that the fatigue strength of 1040 steel material is compatible in terms of increasing load and low cycle number.

REFERENCES

- [1]. Balcıoğlu HE, Sakin R, Dumanay A, Gün H. Development of Fixed-End Type, multi-Sample Flexural Fatigue Test Systems for Composite Plates. *GUSTIJ* (2018) 8 (1): 1-17. 2018;8:1-17. doi:10.17714/gumusfenbil.304488
- [2]. Teknolojileri M, Dergisi E. Manufacturing of Bending Fatigue Test Machine for Flat Shaped Samples. 2015;2015(12):1-11.
- [3]. Gönen D, Oral A, Çakir MC. Design and manufacturing of spring fatigue test device with double compression ratio. 2008;(266):98-108.
- [4]. Cussac P, Gardin C, Pelosin V, et al. Initiation and propagation of fatigue cracks from surface imperfections on 304L austenitic stainless steel. *Procedia Struct Integr.* 2019;19:463-471. doi:10.1016/j.prostr.2019.12.050
- [5]. Blasón S, Poveda E, Ruiz G, Cifuentes H, Fernández Canteli A. Twofold normalization of the cyclic creep curve of plain and steel-fiber reinforced concrete and its application to predict fatigue failure. *Int J Fatigue.* 2019;120(November 2018):215-227. doi:10.1016/j.ijfatigue.2018.11.021
- [6]. Crupi V, Epasto G, Guglielmino E, Squillace A. Influence of microstructure [alpha + beta and beta] on very high cycle fatigue behaviour of Ti-6Al-4V alloy. *Int J Fatigue.* 2017;95:64-75. doi:10.1016/j.ijfatigue.2016.10.002
- [7]. Pessoa DF, Kirchhoff G, Zimmermann M. Influence of loading frequency and role of surface micro-defects on fatigue behavior of metastable austenitic stainless steel AISI 304. *Int J Fatigue.* 2017;103:48-59. doi:10.1016/j.ijfatigue.2017.05.018
- [8]. Sakin R. Investigation of plane-bending fatigue behavior of 1100-H14 aluminum alloy. *J. Fac. Eng. Arch. Gazi Univ.* Vol 25, No 2, 213-223, 2010.
- [9]. Romero C, Yang F, Bolzoni L. Fatigue and fracture properties of Ti alloys from powder-based processes– A review. *Int J Fatigue.* 2018; 117 (June): 407-419. doi:10.1016/j.ijfatigue.2018.08.029
- [10]. Çavdar K, Yılmaz TG. Design and Analysis of Fatigue Test Device for Die Springs. *Uludağ Univ J Fac Eng.* 2017;22(3):163-178. doi:10.17482/uumfd.322853
- [11]. Şik A, Önder M, Korkmaz MS. TaşıtJantlarınınYapısalAnaliz İle Yorulma D ayanımınınBelirlenmesi. *GU J Sci Part:C* 3(3):565-574 (2015)
- [12]. Sengül AB, Çelik A. Fatigue crack growth retardation by the number of different cycles over loading on effect of plasma nitriding. *J Fac EngArchit Gazi Univ.* 2012;27(4).
- [13]. Haghshenas A, Khonsari MM. Damage accumulation and crack initiation detection based on the evolution of surface roughness parameters. *Int J Fatigue.* 2018;107(August 2017):130-144. doi:10.1016/j.ijfatigue.2017.10.009

Hakan GÖKMEŞE, et. al. "Effect of Different Loads on Fatigue Strength of 1040 Steel Materials After Design and Manufacturing of Rotating-Bending Fatigue Test Device." *American Journal of Engineering Research (AJER)*, vol. 9(11), 2020, pp. 121-127.